

A phononic switch based on ferroelectric domain walls

Juan Antonio Seijas-Bellido,¹ Carlos Escorihuela-Sayalero,² Miquel Royo,¹
Mathias P. Ljungberg,³ Jacek C. Wojdel,¹ Jorge Íñiguez,² and Riccardo Rurali¹

¹*Institut de Ciència de Materials de Barcelona (CSIC),
Campus de Bellaterra, 08193 Bellaterra, Barcelona, Spain*

²*Materials Research and Technology Department,
Luxembourg Institute of Science and Technology (LIST),*

5 avenue des Hauts-Fourneaux, L-4362 Esch/Alzette, Luxembourg

³*Donostia International Physics Center, Paseo Manuel de Lardizabal,
4, E-20018 Donostia-San Sebastián, Spain*

(Dated: April 28, 2022)

Abstract

The ease with which domain walls (DWs) in ferroelectric materials can be *written* and *erased* provides a versatile way to dynamically modulate heat fluxes. In this work we evaluate the thermal boundary resistance (TBR) of 180° DWs in prototype ferroelectric perovskite PbTiO₃ within the numerical formalisms of nonequilibrium molecular dynamics and nonequilibrium Green's functions. An excellent agreement is obtained for the TBR of an isolated DW derived from both approaches, which reveals the harmonic character of the phonon-DW scattering mechanism. The thermal resistance of the ferroelectric material is shown to increase up to around 20%, in the system sizes here considered, due to the presence of a single DW, and larger resistances can be attained by incorporation of more DWs along the path of thermal flux. These results, obtained at device operation temperatures, prove the viability of an electrically actuated phononic switch based on ferroelectric DWs.

The modulation of the thermal flux is necessary to encode basic logic functions in devices that operate with heat currents, rather than with charge carriers or electromagnetic waves. This task, however, has thus far been elusive. The reason, simply put, is that phonons, the quantized vibration of the lattice that carry heat in an insulator, have no mass and no bare charge and therefore their motion cannot be easily controlled with an external field¹.

A few configurations, based on heterojunctions^{2,3} or structural asymmetry^{4,5}, have been proposed to implement thermal diodes⁶⁻⁸, where a preferential direction for heat transport exists, i.e. the thermal conductivity depends on the sign of the thermal gradient. A step further, however, would be the design of structures where the thermal conductivity can be *dynamically* tuned. In particular, a system able to reversibly commute between a *low* and a *high* conductivity state would pave the way to digital signal processing with phonons.

Perovskite ferroelectric oxides provide in principle an effective way to pursue this goal. These materials have a spontaneous electric dipole moment determined by the off-center displacement of the cations with respect to the surrounding oxygen cages. Such a polarization can be reoriented or fully reversed with an external electric field, and configurations consisting of juxtaposed domains with different polarization can be designed. Therefore, domain walls (DWs) that separate uniformly-polarized domains can be dynamically and reversibly written and erased. In this work we explore to what extent a specific type of PbTiO_3 DWs, the so-called 180° DWs occurring between adjacent domains of antiparallel orientation of the ferroelectric polarization, act as scattering planes for the incoming phonons, thus yielding a thermal boundary resistance (TBR) that can be switched on and off with an external electric field.

A proof-of-concept of this idea has been experimentally observed in different ferroelectrics and DW configurations. Mante *et al.*⁹ first and Weilert *et al.*^{10,11} later, demonstrated that the thermal conductivity of bulk BaTiO_3 and KH_2PO_4 can be dynamically tuned by electric field alteration of the density of DWs in the material. However, the effect only existed at low temperatures, i.e., as long as phonon-phonon interactions did not become the dominant scattering mechanism. This drawback has been recently overcome with the advent of nanostructured ferroelectrics. Ihlefeld *et al.* have been able to decrease the DW spacing in ferroelectric thin-films made of BiFeO_3 ¹² and $\text{Pb}(\text{Zr}_{0.3}\text{Ti}_{0.3})\text{O}_3$ ¹³ below the average phonon mean free path, which has made it possible to expand the electrically actuated thermal switch operation over a broad temperature range, including room temperature, thus

boosting its potential technological impact.

In spite of the above experimental evidence, a quantitative evaluation of the DWs TBR is missing. Alternatively, this relevant magnitude can be estimated by means of atomistic computational simulations of phonon transport. Nevertheless, for the case of ferroelectric DWs, reports of such simulations are scarce.^{14,15} This can be attributed to the fact that large supercells are required in this type of calculations, which hampers the use of accurate *ab initio* methods, such as density-functional theory (DFT); a second problem relates to the relatively poor transferability and accuracy of the interatomic potential models available nowadays for perovskite oxides. Some of us have recently reported the first study of phonon transport through ferroelectric DWs with atomistic precision.¹⁵ To this end, we obtained the atomic force constants from second-principles model potentials¹⁶ and performed harmonic (ballistic) phonon transport simulations within the nonequilibrium Green’s functions formalism. The calculations revealed an unprecedented polarization-dependent phonon scattering mechanism occurring at PbTiO₃ 180° DWs capable to longitudinally polarize a thermal flux when piercing several DWs. Yet, the harmonic description employed in that study limits, in principle, the validity of the results obtained to the low-temperature and short-channel regimes in which phonon-phonon scattering events can be neglected. In the present paper we go beyond this limitation by performing molecular dynamics simulations – so that we include all orders of anharmonicity in the description of the lattice dynamics – devoted to investigate phonon transport across ferroelectric DWs in the technologically relevant diffusive regime.

We use nonequilibrium molecular dynamics (NEMD) to study the thermal transport properties of PbTiO₃ in mono- and multidomain ferroelectric states at 200 K. To this end, as schematically shown in Fig. 1, we generate a steady state heat flux along the z axis by injecting a certain amount of kinetic energy in a heat source placed at $z = 0$, which is then removed through a heat sink at $z = L_z/2$, where L_z is the size of the simulation supercell along the transport direction¹⁷. The resulting heat flux is calculated as

$$J = \frac{\Delta\epsilon}{2A\Delta t}, \quad (1)$$

where $\Delta\epsilon$ is the energy injected/extracted, A is the supercell cross-section and Δt is the timestep. The thermal conductivity κ is then computed from Fourier’s law after estimating

the thermal gradient that builds up in response to the imposed heat flux

$$\kappa = J/\nabla T. \quad (2)$$

The energy and the forces, as well as the second order force-constants required for the harmonic calculations presented below, of the PbTiO_3 lattice are calculated with the second-principles model potential developed by some of us and thoroughly described in Ref. 16. Within this model the dependence of the lattice energy on the atomic distortions associated with ferroelectricity is expressed as a Taylor series around the paraelectric cubic perovskite structure. More precisely, the energy is conveniently split in three contributions; phonon energy, strain energy and strain-phonon interaction energy, and each one is Taylor expanded as a function of all possible atomic displacements and strains. The series are truncated at 4th order and only pairwise interaction terms, including long-range dipole-dipole interactions, are considered in the model. The potential parameters in the series were either directly determined from first-principles DFT calculation or others, the higher order ones, were fitted to reproduce a training set of relevant lattice-dynamical and structural data (see, e.g., Refs. 16 and 18). The resulting model has repeatedly demonstrated its reliability and predictive power (tested against direct DFT simulations) in a number of works, most of which involved DWs. ^{16,19,20}

We use a $6 \times 6 \times 180$ supercell and a 0.1 fs timestep. Initially we thermalize the system at 200 K by rescaling the velocities of the atoms for 1 ps. When the system is equilibrated, we start the NEMD run by injecting/extracting a certain amount of kinetic energy in the heat source/sink, whose size amounts to 5 unit cells along z . Outside the heat source and sink the system evolves microcanonically. We run 100 ps to reach a nonequilibrium steady-state, with $J_z = 6.3 \cdot 10^{10} \text{ W m}^{-2}$, and then average the temperature over the next 200 ps. The strain, previously determined with a standard equilibrium Monte Carlo calculation at effective temperature of 200 K, is kept fixed in the NEMD simulation. This in principle avoids the need of carrying out the NEMD run in the NPT ensemble.

Our reference system is a PbTiO_3 supercell in its ferroelectric ground-state, i.e., a monodomain configuration with all the ferroelectric distortions pointing along x and, thereby, a continuous polarization P_x developed throughout the simulation box. Far enough from the heat source and sink, the averaged temperature profile is linear as predicted by Fourier's law, with a fitted slope of 4.1 K/nm (see Fig. 2). This estimate, together with the imposed

heat flux, allows us to compute the thermal conductivity from Eq. 2. In this way, we obtain $\kappa_{\text{PTO}} = 16 \text{ W m}^{-1}\text{K}^{-1}$, in good agreement with the self-consistent solution of the Boltzmann transport equation²¹, using 2nd and 3rd order interatomic force constants calculated within the same second-principles model as inputs. Tachibana *et al.*²² experimentally reported a lower value of around $6 \text{ W m}^{-1}\text{K}^{-1}$. However, they report the existence of complex domain structures in their PbTiO_3 samples, thus the true thermal conductivity of the monodomain could be larger. On the other hand, finite size effects, which in general bedevil NEMD simulations^{17,23}, have a negligible effect in our study. We are mostly interested in the TBR, which determines the ratio between the thermal resistance of the high and low conduction states, and has thus a pivotal role in the operation of a potential thermal switch. As we will conclusively prove below, the TBR of the DW here considered is a strictly local property that basically depends on harmonic interactions which have been shown to be properly reproduced by the second-principles model potential.¹⁹

We now move to the case of an individual 180° DW. Notice that, to satisfy periodic boundary conditions, an even number of DWs must be present in the computational cell. Therefore, each calculation will provide two values of the TBR, assessing the error bar of our estimate. As schematically indicated in Fig. 1, the DWs are placed at $z = L_z/4$ and $z = 3L_z/4$. The temperature profile, shown in Fig. 3, features a jump at each DW, the characteristic signature of TBR. A ferroelectric DW is the paradigm of a structurally sharp interface and apparently has a vanishing thickness. The polarization and the temperature change rather abruptly, indeed, but they do so within a finite number of layers of material, as shown in the zoomed view of the inset of Fig. 3. For this reason, we calculate the TBR within a generalized form of the more common Kapitza resistance formalism.²⁴ We proceed as follows. First, we estimate the interface thickness Δz_{DW} by tracking the spontaneous polarization appearing at the DW¹⁹ and perpendicular to the direction of the ferroelectric distortion, P_y ;²⁵ a change of more than two standard deviations from the reference values (far from the DW and the heat source and sink) identify the interface. We obtain an effective thickness of 20 \AA , i.e. 5 unit cells. Next we evaluate the DW temperature, T_s , and the temperatures at the DW boundaries, T_l and T_r (see inset of Fig. 3).

The TBR is then computed within the nonequilibrium thermodynamics formalism^{24,26,27}

by first writing the entropy production due to heat flow at the interface as

$$\sigma^s = J^i \left(\frac{1}{T_s} - \frac{1}{T_l} \right) + J^o \left(\frac{1}{T_r} - \frac{1}{T_s} \right) \quad (3)$$

where J^i (J^o) is the heat flux entering (exiting) the interface. In the stationary state $J^i = J^o = J$ and the corresponding force-flux relations are

$$\frac{1}{T_s} - \frac{1}{T_l} = r^{s,i} J \quad (4)$$

$$\frac{1}{T_r} - \frac{1}{T_s} = r^{s,o} J \quad (5)$$

where, according to the formalism of nonequilibrium thermodynamics, the thermal driving force is the inverse temperature. The TBR is then written as the sum of $r^{s,i}$ and $r^{s,o}$ and reads

$$R_{\text{DW}} = \frac{1}{J} \left(\frac{1}{T_r} - \frac{1}{T_l} \right) T_s^2 = R_s T_s^2 \quad (6)$$

where R_s is the Onsager coefficient for thermal conductivity and the factor T_s^2 is added to recover the dimension of the Kapitza resistance. We obtain a value for R_{DW} of $2.9 \cdot 10^{-10} \text{ K m}^2/\text{W}$.

The TBR adds to the intrinsic thermal resistance of the monodomain, yielding a larger total thermal resistance. Therefore, a DW results in a low conductive state and can be used as the '0' of a phononic binary code. Erasing the DW switches the phononic bit to '1'. The ratio between the high and the low conductive states is obtained dividing the resistance of a segment of material \bar{L} with and without the TBR and reads

$$\frac{R^{\text{high}}}{R^{\text{low}}} = 1 + \frac{R_{\text{DW}}}{\bar{L}/\kappa_{\text{PTO}}} \quad (7)$$

In the setup of Fig. 1, \bar{L} can be as large as $L_z/4 - \Delta z$, but we take the lower value of $\bar{L} = 15.2 \text{ nm}$ to avoid entering the temperature non-linear region next to the heat source and sink (see Fig. 2). With this choice we obtain a ratio $R^{\text{high}}/R^{\text{low}} \sim 1.18$.

We have also calculated the TBR within the nonequilibrium Green's function (NEGF) approach.^{28,29} This scheme is based on the harmonic approximation, hence no phonon-phonon scattering is accounted for and only elastic scattering mechanisms – e.g. associated to impurities or boundaries – are described. This means that a homogeneous perfect crystal, within this approximation, has an infinite thermal conductivity and a length-independent

thermal conductance. Following the NEGF approach we partition the system in three regions: two homogeneous (i.e., DW free) semi-infinite contacts acting as coherent phonon reservoirs and a central scattering region wherein different number of DWs are included. We calculate the thermal conductance due to phonons traveling between the two contacts across the scattering region with the Landauer formula,

$$G(T) = \frac{\hbar}{2\pi\Omega} \int \omega \mathcal{T}(\omega) \left(\frac{\partial n_0(\omega, T)}{\partial T} \right) d\omega. \quad (8)$$

Here, n_0 is the equilibrium Bose-Einstein distribution, Ω is the channel cross section, and \hbar is the reduced Planck constant. Since we assume periodic boundary conditions in the directions perpendicular to the thermal flux, the total phonon transmission function is computed as

$$\mathcal{T}(\omega) = \frac{\Omega}{(2\pi)^2} \int \Xi(\omega, \mathbf{k}_\perp) d\mathbf{k}_\perp, \quad (9)$$

with $\Xi(\omega, \mathbf{k}_\perp)$ being the phonon transmission function calculated at a discrete point (\mathbf{k}_\perp) of the 2D transverse Brillouin zone by means of the Caroli formula,

$$\Xi(\omega, \mathbf{k}_\perp) = \text{Tr} [\mathbf{\Gamma}_L(\omega, \mathbf{k}_\perp) \mathbf{G}_C^r(\omega, \mathbf{k}_\perp) \mathbf{\Gamma}_R(\omega, \mathbf{k}_\perp) \mathbf{G}_C^a(\omega, \mathbf{k}_\perp)]. \quad (10)$$

Here, $\mathbf{G}_C^{r(a)}$ is the retarded (advanced) Green's function of the scattering region which is calculated as

$$\mathbf{G}_C^{r(a)}(\omega, \mathbf{k}_\perp) = \left[\omega^2 \mathbf{I} - \mathbf{H}_C(\mathbf{k}_\perp) - \mathbf{\Sigma}_L^{r(a)}(\omega, \mathbf{k}_\perp) - \mathbf{\Sigma}_R^{r(a)}(\omega, \mathbf{k}_\perp) \right]^{-1}, \quad (11)$$

with \mathbf{I} being the identity matrix, \mathbf{H}_C the second-order force-constant matrix of the atoms in the scattering region, and $\mathbf{\Sigma}_{L(R)}^{r(a)}$ the left (right) contact self-energy. Besides, in Eq. 10, $\mathbf{\Gamma}_{L(R)}$ are broadening functions defined as $\mathbf{\Gamma}_{L(R)}(\omega, \mathbf{k}_\perp) = i \left(\mathbf{\Sigma}_{L(R)}^r(\omega, \mathbf{k}_\perp) - \mathbf{\Sigma}_{L(R)}^a(\omega, \mathbf{k}_\perp) \right)$.

Finally, the self-energies accounting for the coupling between the contacts and the scattering region are calculated as

$$\mathbf{\Sigma}_L^{r(a)}(\omega, \mathbf{k}_\perp) = \mathbf{H}_{C,L}(\mathbf{k}_\perp) \mathbf{g}_L^{r(a)}(\omega, \mathbf{k}_\perp) \mathbf{H}_{L,C}(\mathbf{k}_\perp) \quad (12a)$$

$$\mathbf{\Sigma}_R^{r(a)}(\omega, \mathbf{k}_\perp) = \mathbf{H}_{C,R}(\mathbf{k}_\perp) \mathbf{g}_R^{r(a)}(\omega, \mathbf{k}_\perp) \mathbf{H}_{R,D}(\mathbf{k}_\perp), \quad (12b)$$

where $\mathbf{H}_{\alpha,\beta}$ are force-constant matrices that describe the interaction between the atoms in the contacts and those in the scattering region, and $\mathbf{g}_{L(R)}^{r(a)}$ are the surface contacts Green's functions. The latter are iteratively calculated following the Sancho-Rubio approach.³⁰

The total phonon transmission functions (Eq. 9) for a monodomain and for an individual DW systems are shown in Fig. 4(b). It is observed that the presence of the DW largely suppresses the transmission of phonons with frequencies higher than ~ 40 THz, as would be expected for abrupt interfaces such as the present DW. Nevertheless, a strong scattering is also observed for phonons with frequencies between 10 and 20 THz meaning that the DW does not completely act as a low-pass filter.

Elastic scattering at the DW is the only scattering mechanism captured at this level of the theory, thus the TBR is simply the difference between the thermal resistance of a system with and without a DW. As can be observed in Fig. 4, at temperatures higher than 100 K we obtain an asymptotic TBR value of $2.8 \cdot 10^{-10}$ K m²/W, practically the same value obtained with NEMD at 200 K. The excellent agreement between the length-independent estimate of NEGF and the NEMD simulations, where anharmonic effects are included, implies that (i) the TBR is a local property of the DW; (ii) anharmonic effects play a negligible role in the DW TBR. The DW resistance increases at low temperatures (< 60 K) due to the above mentioned large scattering experienced by the low-energy modes that are excited in this regime.

The possibility of introducing more DWs is very appealing, because it would allow increasing the ratio R^{high}/R^{low} . Therefore, it is interesting to asses to what extent subsequent DWs behave like independent scattering centers with resistances that barely sum up, a sound assumption in a purely diffusive transport regime.³¹ For this reason, we next study the thermal conduction in systems with two DWs. In particular, we consider two cases of DW pairs: in one case the spacing between them is 1.5 nm, in the other 4 nm. We have repeated the procedure described above to define the interface thickness and to calculate the TBR; the final steady state temperature profiles are shown in Fig. 5. In the case of the smaller separation, the DWs *coalesce* making difficult to distinguish two separate interface regions; they are thus treated as one single interface complex. Proceeding in this way we obtain a TBR of $4.7 \cdot 10^{-10}$ K m²/W. When the spacing between the DWs is larger we can treat them individually and we obtain a TBR of $2.3 \cdot 10^{-10}$ K m²/W for each one. In both cases we did not appreciate any difference between parallel or antiparallel orientation of the

spontaneous polarization P_y occurring at the DW.¹⁹

While roughly speaking the thermal resistances of consecutive DWs add up, the obtained TBR per DW is smaller than the value of the individual DW previously calculated. In the low temperature, ballistic transport regime, these DWs have been shown to behave as phonon filters¹⁵ and the presently observed behavior suggest that this effect might partially persist at 200 K and for the specific DW separation here considered. Actually, the total TBR for the system with two separated DWs via NEMD simulations ($4.6 \cdot 10^{-10}$ K m²/W) is larger than the one obtained from the NEGF harmonic calculations ($3.7 \cdot 10^{-10}$ K m²/W). These trends in the additivity of the TBRs indicate that the temperatures and dimensions assumed in our NEMD simulations do not entail a completely diffusive transport, although we can appreciate deviations from the harmonic transport regime.

We have calculated the R^{high}/R^{low} for the configuration with two DWs like in Eq. 7 and taking the same value for \bar{L} ; the contribution from the TBR is now twice $2.3 \cdot 10^{-10}$ K m²/W, while for κ_{PTO} , as in the above discussion for a single DW, we have taken the value obtained in the monodomain configuration. With these assumptions we obtain a value of 1.26. Therefore, by adding more DWs the R^{high}/R^{low} ratio can indeed become larger, but the increase in the case here considered is moderate. The gain R^{high}/R^{low} depends on a delicate balance between design parameters of the system: well spaced DWs entail a large total R_{DW} (approximately n times the TBR of an individual DW, being n the number of DWs), but also a large \bar{L} ; conversely, in a series of nearby DWs \bar{L} can be small, but the TBR per DW could also decrease because of constructive interference and filtering effect.

To summarize, in this paper we have numerically tested the extent to which the simplest type of ferroelectric DWs occurring in PbTiO₃, namely, 180° DWs, behave as barriers for lattice thermal conduction. Our molecular dynamics simulations carried out at relevant temperatures for device operation have shown that the thermal resistance increases by a factor of around 20% due to the presence of a single DW, at the system sizes here considered. This factor can be further increased by incorporating more DWs in the system, though the gain is lower than expected due to the partially non-diffusive nature of thermal transport in the regions between the DWs. We have also demonstrated the local and harmonic character of the DW scattering, as evidenced by the excellent agreement observed among the TBRs from anharmonic NEMD and harmonic NEGF calculations. Our numerical results support the use of ferroelectric domain walls as active mobile elements in electrically actuated thermal

switches.

ACKNOWLEDGMENTS

We acknowledge financial support by the Ministerio de Economía y Competitividad (MINECO) under grant FEDER-MAT2013-40581-P and the Severo Ochoa Centres of Excellence Program under Grant SEV-2015-0496 and by the Generalitat de Catalunya under grants no. 2014 SGR 301. M.R. acknowledges financial support from the Beatriu de Pinós fellowship program (2014 BP_B 00101). C.E.S and J.I. are funded by the Luxembourg National Research Fund through the CORE (Grant C15/MS/10458889 NEWALLS), PEARL (Grant P12/4853155 COFERMAT) and AFR (PhD Grant No. 9934186 for C.E.S.) programs.

-
- ¹ N. Li, J. Ren, L. Wang, G. Zhang, P. Hänggi, and B. Li, *Rev. Mod. Phys.* **84**, 1045 (2012).
² C. Dames, *J. Heat Transfer* **131**, 061301 (2009).
³ R. Rurali, X. Cartoixà, and L. Colombo, *Phys. Rev. B* **90**, 041408 (2014).
⁴ N. Yang, G. Zhang, and B. Li, *Appl. Phys. Lett.* **93**, 243111 (2008).
⁵ X. Cartoixà, L. Colombo, and R. Rurali, *Nano Lett.* **15**, 8255 (2015).
⁶ M. Terraneo, M. Peyrard, and G. Casati, *Phys. Rev. Lett.* **88**, 094302 (2002).
⁷ B. Li, L. Wang, and G. Casati, *Phys. Rev. Lett.* **93**, 184301 (2004).
⁸ N. Roberts and D. Walker, *Int. J. Therm. Sci.* **50**, 648 (2011).
⁹ A. Mante and J. Volger, *Physica* **52**, 577 (1971).
¹⁰ M. A. Weilert, M. E. Msall, J. P. Wolfe, and A. C. Anderson, *Zeitschrift für Phys. B Condens. Matter* **91**, 179 (1993).
¹¹ M. Weilert, M. Msall, A. Anderson, and J. Wolfe, *Phys. Rev. Lett.* **71**, 735 (1993).
¹² P. E. Hopkins, C. Adamo, L. Ye, B. D. Huey, S. R. Lee, D. G. Schlom, and J. F. Ihlefeld, *Appl. Phys. Lett.* **102**, 121903 (2013).
¹³ J. F. Ihlefeld, B. M. Foley, D. A. Scrymgeour, J. R. Michael, B. B. McKenzie, D. L. Medlin, M. Wallace, S. Trolhier-McKinstry, and P. E. Hopkins, *Nano Lett.* **15**, 1791 (2015).
¹⁴ J.-J. Wang, Y. Wang, J. F. Ihlefeld, P. E. Hopkins, and L.-Q. Chen, *Acta Mater.* **111**, 220

- (2016).
- ¹⁵ M. Royo, C. Escorihuela-sayalero, J. Íñiguez, and R. Rurali, Phys. Rev. Mater., accepted.
 - ¹⁶ J. C. Wojdeł, P. Hermet, M. P. Ljungberg, P. Ghosez, and J. Íñiguez, J. Phys. Condens. Matter **25**, 305401 (2013).
 - ¹⁷ P. K. Schelling, S. R. Phillpot, and P. Keblinski, Phys. Rev. B **65**, 144306 (2002).
 - ¹⁸ C. Escorihuela-Sayalero, J. C. Wojdeł, and J. Íñiguez, Phys. Rev. B **95**, 094115 (2017).
 - ¹⁹ J. C. Wojdeł and J. Íñiguez, Phys. Rev. Lett. **112**, 247603 (2014).
 - ²⁰ P. Zubko, J. C. Wojdeł, M. Hadjimichael, S. Fernandez-Pena, A. Sené, I. Luk'yanchuk, J.-M. Triscone, and J. Íñiguez, Nature **534**, 524 (2016).
 - ²¹ W. Li, J. Carrete, N. A. Katcho, and N. Mingo, Comp. Phys. Commun. **185**, 1747 (2014).
 - ²² M. Tachibana, T. Kolodiazny, and E. Takayama-Muromachi, Appl. Phys. Lett. **93**, 092902 (2008).
 - ²³ D. P. Sellan, E. S. Landry, J. E. Turney, A. J. H. McGaughey, and C. H. Amon, Phys. Rev. B **81**, 214305 (2010).
 - ²⁴ R. Rurali, L. Colombo, X. Cartoixa, O. Wilhelmsen, T. T. Trinh, D. Bedeaux, and S. Kjelstrup, Phys. Chem. Chem. Phys. **18**, 13741 (2016).
 - ²⁵ The spontaneous polarization P_x , that defines the ferroelectric ground state, might appear to be a sounder choice. However, it varies more abruptly than P_y , thus we believe the latter better capture the non-bulk nature of a layer of material. Taking the variation P_x to quantify the interface thickness we obtain 12 Å.
 - ²⁶ S. Kjelstrup and D. Bedeaux, in *Non-Equilibrium Thermodynamics of Heterogeneous Systems*, Vol. 16 (World Scientific, Singapore, 2008).
 - ²⁷ R. Dettori, C. Melis, X. Cartoixa, R. Rurali, and L. Colombo, Adv. Phys. X **1**, 246 (2016).
 - ²⁸ M. Pourfath, *The Non-Equilibrium Green's Function Method for Nanoscale Device Simulation* (Springer, 2014).
 - ²⁹ S. Sadasivam, Y. Che, Z. Huang, L. Chen, S. Kumar, and T. S. Fisher, Ann. Rev. Heat Transfer **17**, 89 (2014).
 - ³⁰ M. L. Sancho, J. L. Sancho, and J. Rubio, J. Phys. F: Met. Phys. **14**, 1205 (1984).
 - ³¹ S. Lu and A. J. H. McGaughey, AIP Advances **5**, 053205 (2015).

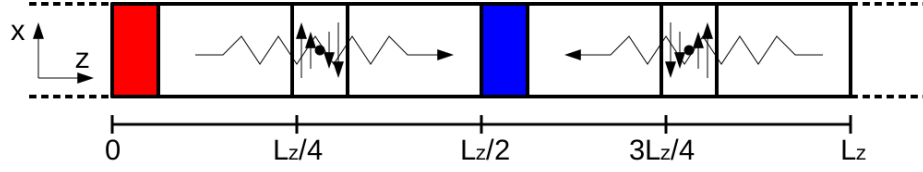


FIG. 1. Schematic view of the supercell for a simulation in which thermal transport through two independent DWs is evaluated. The red and blue rectangles illustrate the position of the thermal source and sink, respectively, and the transport directions are indicated with horizontal arrows.

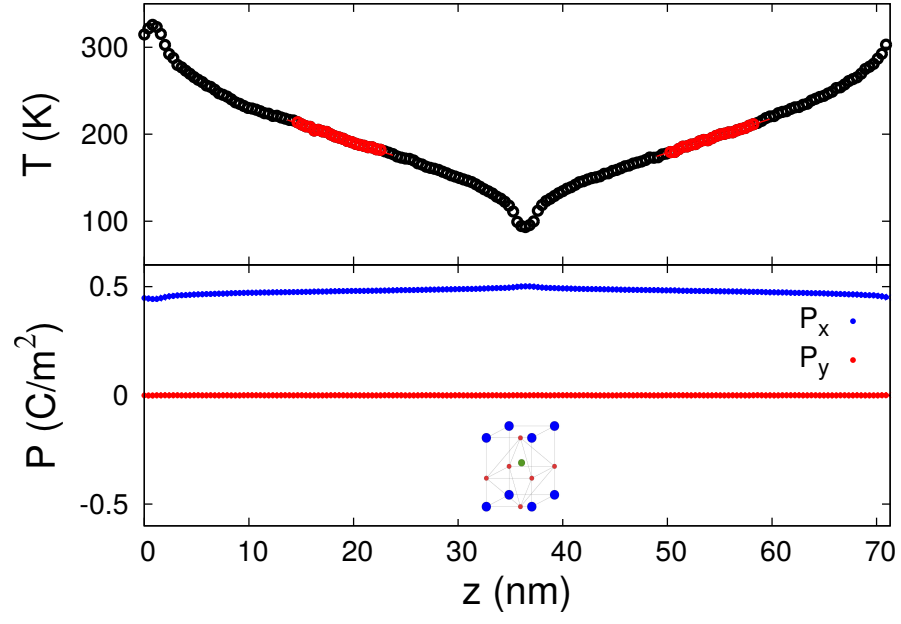


FIG. 2. (Top) Temperature and (bottom) polarization profiles along the transport direction z for the case of a monodomain PbTiO_3 . Heat flows from the heat source at $z = 0$ to the heat sink at $z = 35$ nm. Data in red are used to fit the thermal gradient. The uniform ferroelectric distortion is sketched in the inset of the bottom panel.

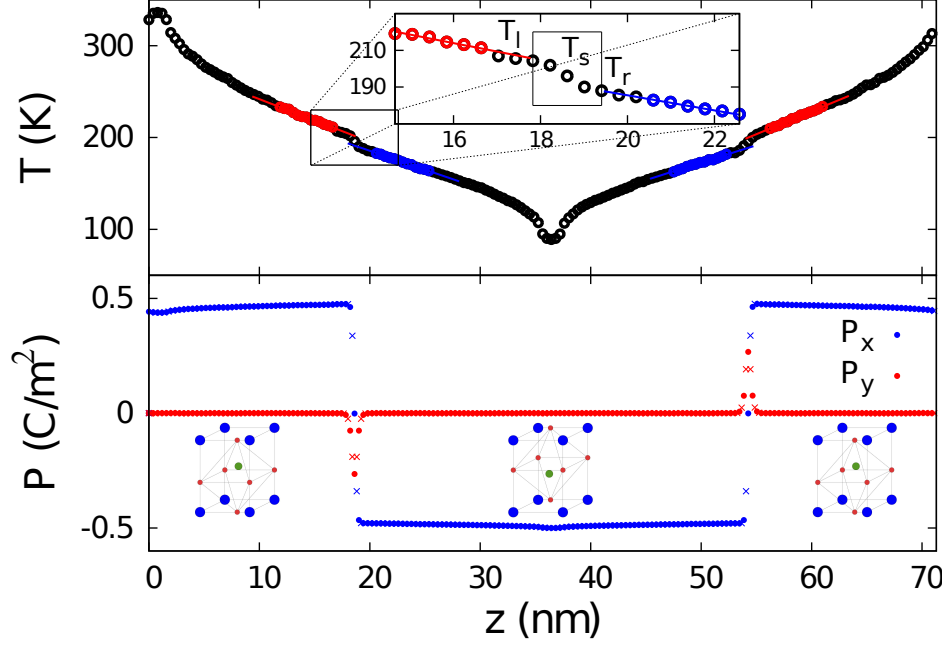


FIG. 3. (Top) Temperature and (bottom) polarization profiles along the transport direction z for the case with one DW. Heat source and sink are placed like in Fig. 2 and the DWs are at ~ 17 and ~ 52 nm. The inset of the top panel shows a zoomed view of the temperature profile at one of the DW; the relevant temperatures used to calculate the TBR are indicated.

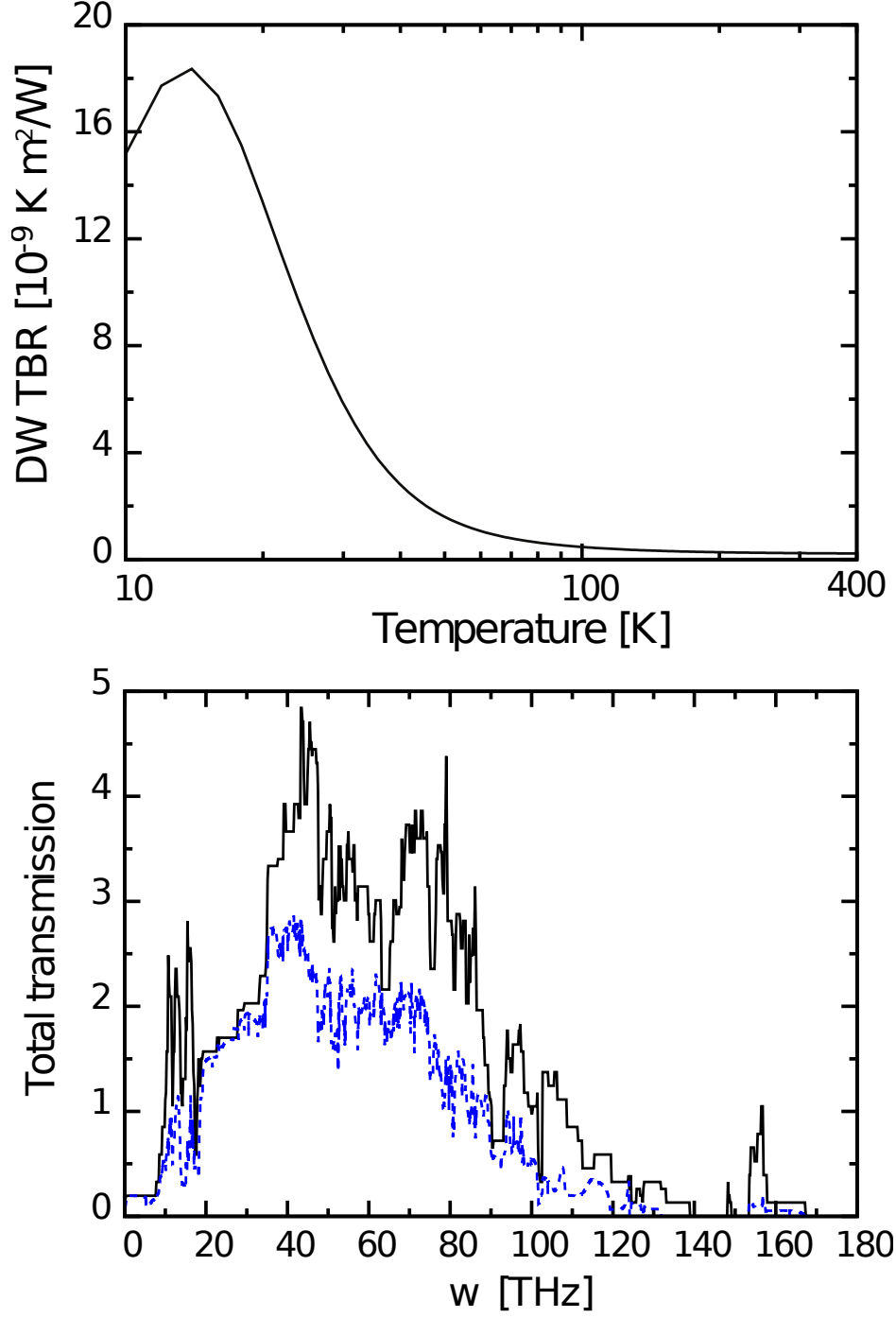


FIG. 4. (Top) TBR as a function of temperature computed within the harmonic NEGF approach as, $G_{DW}^{-1} - G_{mono}^{-1}$, where G_{DW} (G_{mono}) is the thermal conductance of the case with (without) DW. (Bottom) Phonon transmission as a function of frequency for the case of a monodomain (continuous line) and a DW (dashed line).

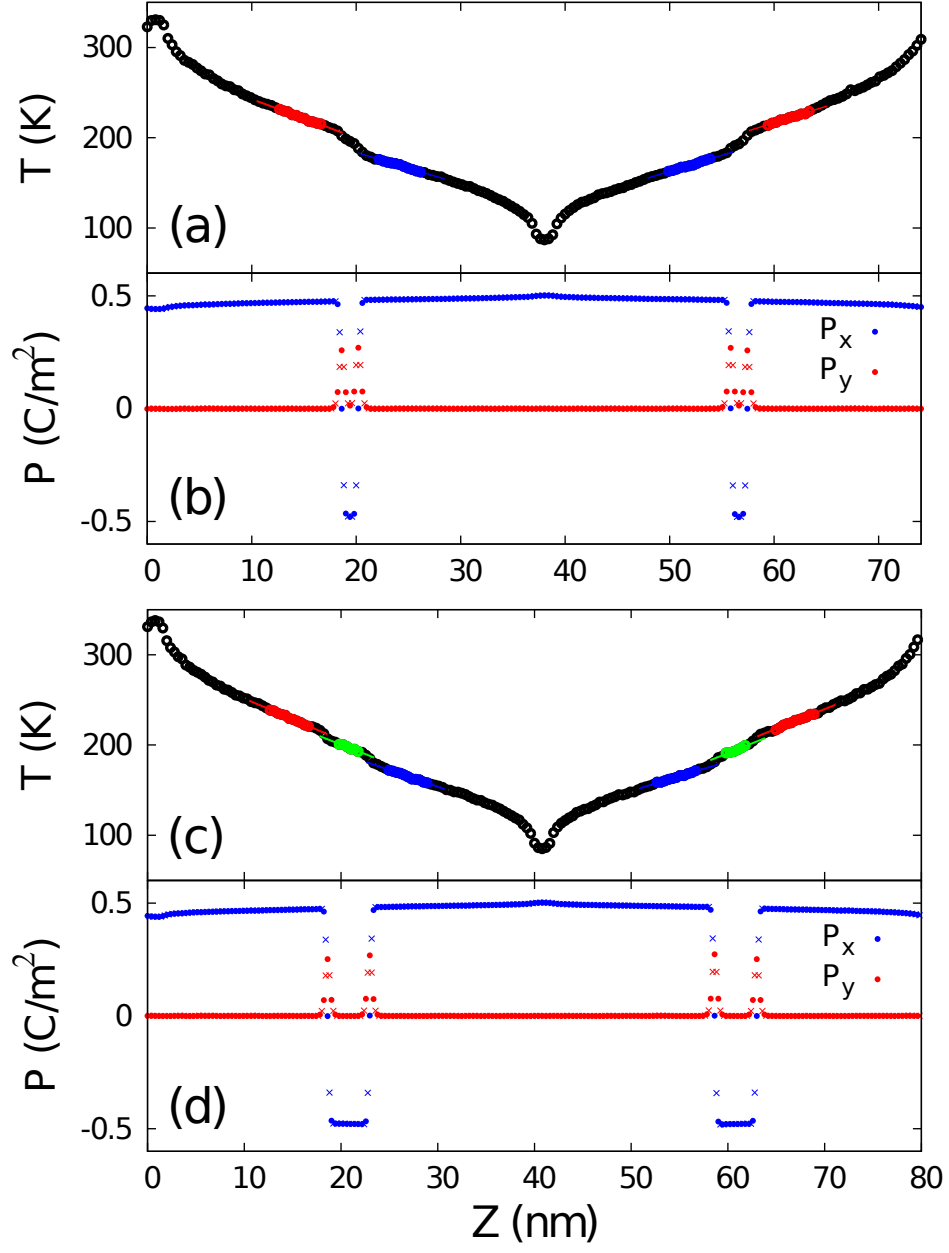


FIG. 5. Temperature and polarization profiles along the transport direction z for the cases with two DWs separated by ~ 1.5 nm, (a) and (b), and ~ 4 nm, (c) and (d).